

# Comparison of the Plasma-Photocatalyst Synergy at Low and Atmospheric Pressure

F. Thevenet<sup>1,2</sup>, O. Guaitella<sup>1</sup>, C. Guillard<sup>2</sup>, E. Puzenat<sup>2</sup>, G. Stancu<sup>3</sup>, J. Roepcke<sup>3</sup> and A. Rousseau<sup>1\*</sup>

<sup>1</sup> LPTP, Ecole Polytechnique, CNRS, Palaiseau, France

<sup>2</sup> IRCELYON, Institut de recherches sur la catalyse et l'environnement de Lyon, CNRS, Lyon, France.

<sup>3</sup> INP-Greifswald, Greifswald, Germany.

**Abstract** - The decay rate of C<sub>2</sub>H<sub>2</sub> in a plasma-photocatalyst coupling device is analyzed at atmospheric pressure and in a pulsed low pressure DC discharge. In the latter case, mid infrared laser absorption spectroscopy of the gas phase makes possible the dynamic measurement of the C<sub>2</sub>H<sub>2</sub> density in a single plasma shot with a time resolution of 1 ms. Plasma-TiO<sub>2</sub> combination for VOC is shown and an addition synergistic effect is evidenced when external ultraviolet radiation are added. At atmospheric pressure, gas phase and adsorbed phase analyses have been performed in order to evaluate the oxidation processes performances regarding to the pollutant removal and the selectivity into CO and CO<sub>2</sub>.

**Keywords** - Plasma-photocatalyst coupling; VOC removal, Laser absorption spectroscopy.

## 1. INTRODUCTION

Indoor air cleaning has become a new technological challenge for odors or diluted pollutant removal. Photocatalysis is based on the oxidation of molecules on the surface of a porous semiconductor material illuminated with ultraviolet radiation; the main advantage of this technique is that it can lead to the complete oxidation of Volatile Organic Compounds (VOC) to CO<sub>2</sub> and salts.

The fact that only UV sources supply is required to perform photocatalysis has to be noticed since it represents a significant energy saving in comparison to thermal catalysis. Moreover, photocatalysis exhibits a high oxidation ability for each type of VOC. Its efficiency has been demonstrated even with triple carbon-carbon bonding, as recently reported by Thevenet et al. [1] for acetylene photocatalytic oxidation.

It was recently shown that the combination of photocatalytic material with non-thermal plasma activates the oxidation process [2-13]. The synergy between the plasma and the photocatalytic material leads to a higher CO<sub>2</sub>/CO ratio (selectivity), as well as a better oxidation efficiency. So far, the physico-chemical processes of the synergy are rarely investigated and not understood.

When TiO<sub>2</sub> is immersed in the plasma, it is irradiated by the ultraviolet generated by excited nitrogen molecules, and bombed by charged particles, metastable states, and O and N atoms. Unfortunately, atmospheric pressure plasmas are strongly non-uniform, which makes direct in-situ measurements almost impossible. To overcome this problem, we have recently suggested to use a pulsed *low pressure* DC discharge, which is spatially uniform. This allows to study the plasma-photocatalyst interaction using in situ time resolved optical diagnostics; the influence of TiO<sub>2</sub> pellets on the O atom production in a pulsed low

pressure DC discharge was recently reported [14]; and the time evolution of C<sub>2</sub>H<sub>2</sub> in a *single shot* pulsed plasma was measured by Tuneable Diode Laser Absorption Spectroscopy (TDLAS) in the infrared region [15]. This gave some insight into the plasma-photocatalyst synergy by measuring the time evolution of C<sub>2</sub>H<sub>2</sub> under plasma exposure, with or without TiO<sub>2</sub> pellets, with or without additional ultraviolet irradiation.

An other advantage is that steady state DC discharges have been extensively studied by Gordiets *et al.* [16] and Smirnov *et al.* [17] in fairly similar conditions, giving a useful database for plasma parameters such as the reduced electric field, plasma density and temperature.

In the present article, we first report the comparison between the characteristic time of C<sub>2</sub>H<sub>2</sub> removal in an atmospheric DBD discharge and in a pulsed low pressure DC discharge. We also investigate the plasma-photocatalyst coupling at atmospheric pressure from a reaction pathway point of view by reporting main reaction intermediates and by-products.

## 2. EXPERIMENTAL

Two types of plasma reactor, devoted to the plasma-photocatalyst coupling, are studied.

### 2.1 ATMOSPHERIC PRESSURE REACTOR

The coupling of plasma-photocatalysis has been studied in a specially designed Pyrex glass reactor allowing a plan to plan geometry [18]. The active part of the system consists in a rectangular section channel. Copper electrodes are deposited on each side of the largest walls of the channel and connected to a high voltage supply. The high voltage of 50 Hz frequency ranges from 0 to 25kV.

\* Corresponding author : Antoine Rousseau  
e-mail address : Antoine.Rousseau@lptp.polytechnique.fr

Originally presented at ISNTPT-5, June 2006

Revised; January 29, 2007, Accepted; February 15, 2007

The plasma injected power is calculated by Lissajou plot method [19]. The gas gap between the dielectric is 6mm wide. Dry synthetic air, containing a controlled amount of organic volatile pollutant, can flow through this space. The photocatalytic material selected for the coupling consists in silica fibres coated with 20g/m<sup>2</sup> of colloidal silica ensuring the fixation of 20g/m<sup>2</sup> of P25-Degussa titanium dioxide nanoparticles. It is later named Si20Ti20. Materials preparation have been performed by *Ahlstrom Research and Services*. If experiment requires photocatalytic material, the material is cleaned during 30min under dry synthetic air flow and UV light before operating. Four external Philips PLL40 UV lamps are placed around the reactor in order to illuminate Si20Ti20 materials, placed in the reactor, from the outer part. Experiments have been carried out in a recirculation mode in order to compare the kinetics of the processes and the evolution of volatil compound concentration as a function of time and others parameters depending on time like injected energy. The recirculation flow is 200mL.min<sup>-1</sup> and is ensured by a pump. The total volume of the batch reactor is 1.5L, which lead to a 3s residence time considering a single pass.

The presence of a material inside the discharge clearly increases the injected energy at constant voltage. In order to perform experiments at the same injected energy which is the parameter governing the reactivity of the system, the voltage is adjusted, and all the experiments at atmospheric pressure have been carried out at the same injected power.

## 2.2 ANALYTICAL DEVICES FOR ATMOSPHERIC PRESSURE EXPERIMENTS

Gas phase analyses are performed ex-situ and adsorbed phase analyses are performed after the coupling experiments. C<sub>2</sub>H<sub>2</sub>, CO and CO<sub>2</sub>, are monitored by Varian gas phase chromatograph. Acetylene is detected by flame ionization (FID), whereas CO and CO<sub>2</sub> are first converted into methane over Ni catalyst under hydrogen flow and then analyzed by FID. In the gas phase, carboxylic acids have been analyzed and quantified. They have been solubilized into pure acidic water and have been analyzed by HPLC equipped with a sarasep-car-H column and a UV detector (210 nm). Gaseous aldehydes have been investigated too. Derivation cartridges containing 2,4 dinitrophenylhydrazine have been placed at the outlet of the reactor. After desorption, hydrazones are analyzed by convenient HPLC equipments. Finally, carboxylic acids, adsorbed on materials placed inside the discharge during coupling, have been desorbed, identified and quantified by appropriate HPLC device.

## 2.3 LOW PRESSURE PLASMA

The pulsed discharge was ignited in a 47 cm long (59 cm optical length) and 2.1 cm inner diameter pyrex tube [15]. The DC pulsed generator delivered a current of 3 mA, with a pulse duration of 1 s. Commercially available TiO<sub>2</sub>

pellets (20g of pure anatase, Alfa Aesar #43828, size specific surface 37 m<sup>2</sup>/g) were placed inside the discharge tube. Experiments were performed under static conditions: dry synthetic air N<sub>2</sub>/O<sub>2</sub> = 80/20 % (< 3 ppm of H<sub>2</sub>O and 0,5ppm of hydrocarbons) was first pre-mixed to reach 900 ppm C<sub>2</sub>H<sub>2</sub> in a buffer volume, the discharge tube being pumped down to a base pressure of less than 5 Pa. The pre-mixed gas was then injected into the discharge tube, which was closed when the pressure reached 210 Pa. In order to check the influence of external ultraviolet radiation, two mercury lamps (Philips PL-L 24W/10/4P) were mounted parallel to the discharge tube axis.

## 2.4 ANALYTICAL DEVICE FOR LOW PRESSURE EXPERIMENTS

In-situ single path laser absorption spectroscopy is performed on C<sub>2</sub>H<sub>2</sub> molecules through the discharge tube. The infrared diode laser is a helium cooled IRMA, described in Röpcke et al. [20], which may be externally triggered and provides a pulse resolution of 0.46 ms. C<sub>2</sub>H<sub>2</sub> density is deduced from Beer's law:

$$I(\nu) = I_0(\nu) \exp[-k(\nu)L] \quad (1)$$

where I(ν) is the transmitted radiation intensity, I<sub>0</sub>(ν) is the incident intensity on the sample, k(ν) is the absorption coefficient per unit length and L is the total absorption path length. The integrated absorption coefficient over frequency, K<sub>ν</sub>, for a homogeneous sample is

$$K_\nu = \int_\nu k(\nu) d\nu = \frac{1}{L} \int_\nu \ln\left(\frac{I_0}{I}\right) d\nu = N S(T) \quad (2)$$

where N is the total density of the absorbing species; S(T) is the line strength of the rovibronic transition used for species measurement. The temperature increase during the plasma pulse was estimated to be less than 50°C using the thermal diffusion equation; hence, the temperature dependency of S(T) was neglected. The strong transition of C<sub>2</sub>H<sub>2</sub> at 771.404 cm<sup>-1</sup> has been used in the present work. The IRMA system measured the integrated absorption coefficients and then, by using the line strength value, absolute concentrations were obtained.

The steady state density of C<sub>2</sub>H<sub>2</sub> is about 900 ppm, without TiO<sub>2</sub> pellets inserted inside the discharge tube. On the contrary, when the discharge tube is filled with the pre-mixed gas in the presence of TiO<sub>2</sub> pellets, its steady state density is only 580 ppm. This means that about 36 % of the injected C<sub>2</sub>H<sub>2</sub> is adsorbed on the TiO<sub>2</sub> pellets with a characteristic adsorption time of about 3.5 s. Let us note that N<sub>2</sub>/O<sub>2</sub> molecules are not adsorbed since no pressure drop is measured during C<sub>2</sub>H<sub>2</sub> adsorption. At the steady state about 47 % have disappeared from the gas phase, which is notably higher than without UV pre-irradiation. Such a pre-irradiation effect lasts for more than 20 s (time between pre-irradiation and filling of the discharge tube).

### 3. RESULTS

#### 3.1 ATMOSPHERIC PRESSURE REACTOR

Fig. 1 shows the time evolution of  $C_2H_2$  in the atmospheric pressure plasma reactor.

Four conditions are tested : i) photocatalysis only (photocatalytic material + UV), ii) plasma only, iii) plasma + photocatalytic material, iv) plasma + photocatalytic material + UV.

The main observation is the slow kinetics of photocatalysis regarding to plasma process. Plasmas performed for this part of the experiments are 0,2W. The first decay rate obtained with photocatalytic process is  $5.6 \times 10^{-5} \text{ s}^{-1}$  (table 1), whereas it reaches  $18 \times 10^{-5} \text{ s}^{-1}$  with plasma process. Nevertheless, attention has to be paid to the mineralization rate : photocatalytic treatment leads to the formation of  $CO_2$  (90 % of the carbon balance) and  $CO$  (9 % of the carbon balance). By-products, mainly adsorbed carboxylic acids, correspond to less than 1 % of the carbon balance. On the contrary, cumulated quantities of  $CO$  and  $CO_2$  do not exceed 50 % of the carbon balance even after 4 h of plasma treatment. Intermediates and by-products are numerous. Acetaldehyde, formaldehyde, glyoxal and formic acids have been mainly identified in the gas phase.

TABLE 1

First decay rate coefficients observed during acetylene elimination at (i) low and (ii) atmospheric pressure for the four experimental conditions.

Case	Cconditions	1 <sup>st</sup> decay rate ( $s^{-1}$ )	
		low Pressure	atm. Pressure
a	$TiO_2 + UV$	0.33	$5.6 (x 10^{-5})$
b	plasma	20.8	$18 (x 10^{-5})$
c	plasma + $TiO_2$	22.2	$29 (x 10^{-5})$
d	plasma + $TiO_2 + UV$	30.3	$37 (x 10^{-5})$

The presence of Si20Ti20 coated glass fibres inside the discharge modifies the first decay rate which is strongly improved and reaches  $29 \times 10^{-5} \text{ s}^{-1}$  for plasma coupled with Si20Ti20 (plasma+Si20Ti20). Kim et al [21] suggest that material surface, especially titanium dioxide, can be activated by high energy particles such as electrons, excited molecules or radicals. Roland et al. [22] suggest that such removal improvements are related to the porosity of the structure. Porosity would induce a longer residence time of gas species during diffusion through the solid pore system. They also noticed a significant role of ozone, produced by DBD, interacting with material surface. This hypothesis has to be taken into account with titanium dioxide since a positive effect of ozone on organic compound photocatalytic oxidation is reported [23]. In our experiment, a decrease of the ozone concentration when  $C_2H_2$  is added in the reactor may be attributed to the ozone consumption due to  $C_2H_2$  oxidation. On the other hand,

this reduction may also be due to the decrease of ozone precursors such as O atoms.

As noticed by Kim et al. [21], part of plasma energy is converted into UV light. Although being small in their intensity, photocatalysis could be performed inside the plasma without classical UV lamps. Nevertheless, we noticed that  $CO$  and  $CO_2$  selectivities are slightly decreased by the presence of the material. Gaseous carboxylic acids and aldehydes are identified in the same proportions than without material, and carboxylic acids containing from 1 to 4 carbon atoms have been evidenced on material surface ( $C_2$  and  $C_3$  are the main structures). In order to determine if plasma UV and excited species significantly activate photocatalytic titanium dioxide particles, experiments have been carried out with an equivalent non-photocatalytic material : silica fibres are only coated by  $40 \text{ g/m}^2$  of colloidal silica. Performances observed are the same, indicating that the photocatalytic properties of the Si20Ti20 material are not involved into

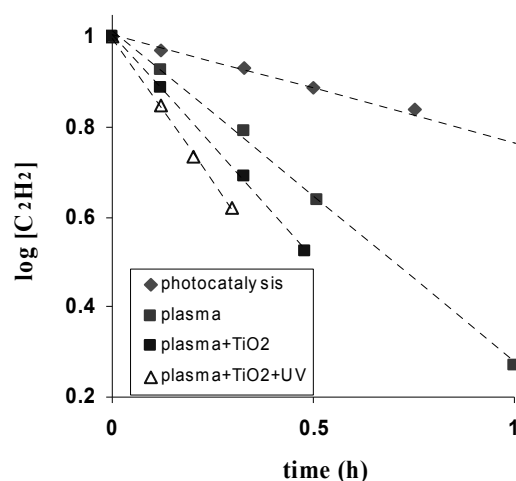


Fig. 1. Decay of  $C_2H_2$  in the atmospheric pressure reactor (recycling). The plasma is a planar DBD and photocatalytic material is located inside the plasma region. Measurements are performed using Gas Chromatography

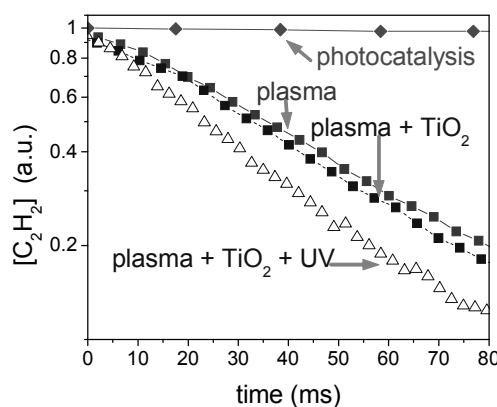


Fig. 2. Decay rate of  $C_2H_2$  in a pulsed low pressure DC discharge. Measurements are performed in single plasma shot in situ, using time resolved measurement absorption spectroscopy in the mid infrared region.

the plasma-material positive interaction. Additional UV lamps seem to be necessary to take part of photoactivity.

First decay rate reaches  $37 \times 10^{-5} \text{ s}^{-1}$  if Si20Ti20 material is irradiated inside the discharge. Moreover, this improvement is correlated to a significant increase of  $\text{CO}_2$  selectivity. Two reasons can explain this synergetic effect. First, the classical photocatalytic process is induced by the UV light, but the improvement we observed exceeds the performances of photocatalysis evaluated above. Then we can consider that photocatalysis is also effective for plasma by-products oxidation (mainly the adsorbed one).

This hypothesis is confirmed that the distribution of the carboxylic acids molecular weight adsorbed on the material. In the presence of UV light, carboxylic acids containing 1 carbon atom are the major detected adsorbed acids. Percentages of carbon balance represented by carboxylic acids detected on Si40 and Si20Ti20 materials under 0.2 W, UV-irradiated or not, are reported in Figure 3. In presence of pure silica (Si40 material) carboxylic acids represent 0.25 (+/-0,1) % (of the carbone balance. This value is not modified when the material is irradiated by additional UV lamps; corresponding to the fact that silica is not sensitive to UV photons.

Non irradiated photocatalytic material (Si20Ti20) leads to an amount of carboxylic acids corresponding to 0.6 (+/-0.1) % of the carbon balance, exceeding the amount detected on Si40 material. This difference cannot be related to the specific surface of the materials: on the contrary, Si20Ti20 is  $20.6 \text{ m}^2/\text{g}$  and Si40 is  $28,3 \text{ m}^2/\text{g}$ . It could be suggested that materials, depending on their chemical nature, can enhance or not the recombination of radicals on their surface. This hypothesis would deserve further precise investigations.

When Si20Ti20 material is UV-irradiated the percentage of carbon balance corresponding to carboxylic acid is multiplied by 4.5. Two acids are mainly favoured: the amounts of acetic and oxalic acids are both multiplied by ten. Formic acid is also significantly improved. We suggest that photocatalytic properties of UV-irradiated Si20Ti20 are responsible for the observed phenomenon. Adsorbed acids could be considered as photocatalytic oxidation by products of other organic compounds. Plasma generates numerous unstable intermediates which can get stabilized either on the porous surface, forming alcohols or aldehydes, or in the gas stream flowing through the fibrous material. Those organic species could be photooxydized by irradiated  $\text{TiO}_2$ . Photocatalytic oxidation of alcohols, aldehydes and ketones lead to the formation of carboxylic acids, as intermediates [23-24].

### 3.2. LOW PRESSURE IN SITU MEASUREMENT

Figure 2 shows the time evolution of  $\text{C}_2\text{H}_2$  during the first 250 ms for different experimental conditions plotted in semi-log scale; Most of the curves show a bi-exponential decay with the corresponding characteristic rate coefficient listed in Table 1. The change of the slope

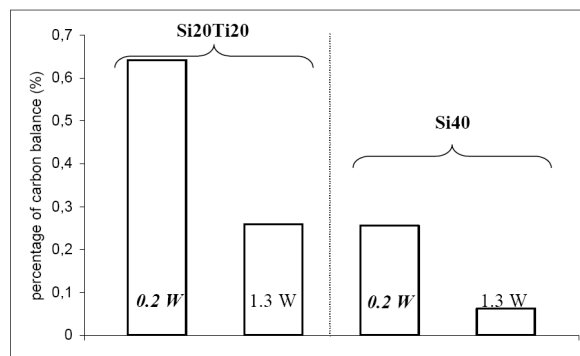


Fig. 3. Percentage of carbon balance represented by carboxylic acids detected on Si40 ad Si20Ti20 materials under 0.2 W discharges with and without UVs (gas flow = 500 sccm,  $[\text{C}_2\text{H}_2] = 1000 \text{ ppm}$ , in cylindrical DBD).

occurs when nearly 90% of the initial  $\text{C}_2\text{H}_2$  amount is removed. It means that at this stage of the oxidation process the composition of the reactor atmosphere is dramatically different in comparison with the initial stage. This can modify the reactivity and the adsorption ability of the various compounds of the gas phase leading to different kinetics and therefore a different slope. For case b (plasma only), the rate coefficient is reduced by a factor 3 (from  $20.8$  to  $7 \text{ s}^{-1}$ ) about 100 ms after the beginning of the pulse. The electron density and reduced electric field being roughly constant during the pulse, such an effect must be attributed to gas phase kinetics between neutrals.

When a photocatalytic surface is inserted inside the plasma region, the decay time decreases only by 37 % (from  $22.2$  to  $14 \text{ s}^{-1}$ ). This may be due to surface oxidation of  $\text{C}_2\text{H}_2$  and/or to a modification of the density of oxidative radicals and molecules in the gas phase.

The presence of photocatalytic pellets leads to a very small increase of the first rate coefficient from  $20.8$  to  $22.2 \text{ s}^{-1}$  (case b, c). This shows that, for the low pressure conditions studied here, the plasma alone cannot efficiently activate  $\text{TiO}_2$ . It was recently shown that under similar experimental conditions the reduced electric field  $E/N$  increases from 80 to 92 Td when porous  $\text{TiO}_2$  surface is inserted inside the plasma region.<sup>18</sup> From Fig. 2 we conclude that  $\text{C}_2\text{H}_2$  destruction in the gas phase is not controlled by electron impact dissociation, since an increase of electron energy has no definite influence on the  $\text{C}_2\text{H}_2$  destruction rate coefficient.

The most interesting result is the strong synergetic effect obtained when the plasma is combined with  $\text{TiO}_2$  pellets with external UV irradiation (case d). The 1<sup>st</sup> rate coefficient is increased from  $22.2 \text{ s}^{-1}$  in the case of plasma /  $\text{TiO}_2$  combination (case c) to  $30.3 \text{ s}^{-1}$  when external UV irradiation is added (case d); this represents a 36 % increase of the  $\text{C}_2\text{H}_2$  rate coefficient. Hence the photocatalytic effect of  $\text{TiO}_2$  irradiated with UV is strongly enhanced when non-thermal plasma is added: the rate coefficient increases from  $0.33 \text{ s}^{-1}$  (case a), to  $30.3 - 22.2 = 8.1 \text{ s}^{-1}$  (case d). This represents a multiplying factor of 25 .

#### 4. CONCLUSION

We have studied in parallel the synergy of the plasma-photocatalyst coupling at low pressure and at atmospheric pressure.

- 1) First, the ordering of the different contribution is the same at low and high pressure, which legitimates our original approach.
- 2) The key point in the plasma photocatalyst coupling is the respective influence of the porosity of the material versus its photocatalytic activity. At atmospheric pressure, the interaction between the plasma and the material porosity clearly enhances the elimination of acetylene. The mineralization into CO and CO<sub>2</sub> can be improved by additional irradiation of the photocatalyst.

#### REFERENCES

- [1] F. Thevenet, O. Guaitella, J.-M. Herrmann, A. Rousseau, C. Guillard, "Photocatalytic degradation of acetylene over various titanium dioxide-based photocatalysts", *Appl. Catal. B: Environ.*, vol. 61, pp. 58-68, 2005.
- [2] A. Ogata, H. Einaga, H. Kabashima, S. Futamura, S. Kushiyama and Hyun-Ha Kim, "Effective combination of nonthermal plasma and catalysts for decomposition of benzene in air", *Appl. Catal. B: Environ.*, vol. 46, pp. 87-95, 2003.
- [3] A. Ogata, H. H. Kim, S. Futamura, S. Kushiyama and K. Mizuno, "Effects of catalysts and additives on fluorocarbon removal with surface discharge plasma", *Appl. Catal. B: Environ.*, vol. 53, pp. 175-180, 2004.
- [4] B.Y. Lee, S.H. Park, S.C. Lee, M. Kang and S.-J. Choung, "Decomposition of benzene by using a discharge plasma-photocatalyst hybrid system", *Catal. Today*, vol. 93, pp. 769-776, 2004.
- [5] D. Li, D. Yakushiji, S. Kanazawa, T. Ohkubo, Y. Nomoto, "Decomposition of toluene by streamer corona discharge with catalyst", *J. Electrostat.*, vol. 55, pp. 311-319, 2002.
- [6] H. H. Kim, K. Takashima, S. Katsura and A. Mizuno, "Low-temperature NO<sub>x</sub> reduction processes using combined systems of pulsed corona discharge and catalysts", *J. Phys. D: Appl. Phys.*, vol. 34, pp. 604-613, 2001.
- [7] K. Krawczyk and M. Mlotek, "Combined plasma-catalytic processing of nitrous oxide", *Appl. Catal. B: Environ.*, vol. 30, pp. 233-245, 2001.
- [8] M. Dors and J. Mizeraczyk, "NO<sub>x</sub> removal from a flue gas in a corona discharge-catalyst hybrid system", *Catal. Today*, vol. 89, pp. 127-133, 2004.
- [9] M. Kang, B.-J. Kim, S. M. Cho, C.H. Chung, B.W. Kim, G.Y. Han and K.J. Yoon, "Decomposition of toluene using an atmospheric pressure plasma/TiO<sub>2</sub> catalytic system", *J. Molec. Catal. A: Chem.*, vol. 180, pp. 125-132, 2002.
- [10] S. Kameoka, T. Kuriyama, M. Kuroda, S. Ito, K. Kurimori, "The chemical interaction between plasma-excited nitrogen and the surface of titanium dioxide", *Appl. Surf. Sci.*, vol. 89, pp. 411-415, 1995.
- [11] S. Futamura, H. Einaga, H. Kabashima and L.Y. Hwan, "Synergistic effect of silent discharge plasma and catalysts on benzene decomposition", *Catal. Today*, vol. 89, pp. 89-95, 2004.
- [12] S. Bröer and T. Hammer, "Selective catalytic reduction of nitrogen oxides by combining a non-thermal plasma and a V<sub>2</sub>O<sub>5</sub>-WO<sub>3</sub>/TiO<sub>2</sub> catalyst", *Appl. Catal. B: Environ.*, vol. 28, pp. 101-111, 2000.
- [13] T. Hammer, T. Kappes and M. Baldauf, "Plasma catalytic hybrid processes: gas discharge initiation and plasma activation of catalytic processes", *Catal. Today*, vol. 89, pp. 5-14, 2004.
- [14] O. Guaitella, L. Gatilova, A. Rousseau, "Plasma-photocatalyst interaction: Production of oxygen atoms in a low pressure discharge", *Appl. Phys. Lett.*, vol. 86, 151502, 2005.
- [15] A. Rousseau, O. Guaitella, L.V. Gatilova, F. Thevenet, C. Guillard, J. Roepcke, G. D. Stancu, "Photocatalyst activation in a pulsed low pressure discharge", *Appl. Phys. Lett.*, vol. 87, 221501, 2005.
- [16] B.F. Gordiets, C.M. Ferreira, V.L. Guerra, J.M.A.H. Loureiro, J. Nahorny, D. Pagnon, M. Touzeau, M. Vialle, "Kinetic model of a low-pressure N<sub>2</sub>-O<sub>2</sub> flowing glow discharge", *IEEE Trans. Plasma Sci.*, vol. 23, pp. 750-768, 1995.
- [17] S.A. Smirnov, V.V. Rybkin, I.V. Kholodov, "Simulation of the Processes of Formation and Dissociation of Neutral Particles in Air Plasma: Vibrational Kinetics of Ground States of Molecules", *High Temp.*, vol. 40, No. 2, 2002.
- [18] F. Thevenet, O. Guaitella, E. Puzenat, C. Guillard, J.-M. Herrmann, A. Rousseau, (*in press*) "Oxidation of acetylene by photocatalysis coupled with dielectric barrier discharge" *Catal. Today*, 2007.
- [19] T.C. Manley, *Trans. Electrochem. Soc.*, vol. 84, pp. 83-96, 1943.
- [20] J. Röpcke, L. Mechold, M. Käning, J. Anders, F.G. Wienhold, D. Nelson and M. Zahniser, "A tunable infrared multicomponent acquisition system for plasma diagnostics", *Rev. Sci. Instr.*, vol. 71, pp. 3706-3710, 2000.
- [21] H.-H. Kim, Y.-H. Lee, A. Ogata, S. Futamura, "Plasma-driven catalyst processing packed with photocatalyst for gas-phase benzene decomposition", *Catalysis Communication*, vol. 4, pp. 347-351, 2003.
- [22] U. Roland, F. Holzer, F.-D. Kopinke, "Improved oxidation of air pollutants in a non-thermal plasma", *Catal. Today*, vol. 73, pp. 315-323, 2002.
- [23] M.-L. Sauer, D.-F. Ollis, "Photocatalyzed Oxidation of Ethanol and Acetaldehyde in Humidified Air", *J. Catal.*, vol. 158, pp. 570-582, 1996.
- [24] J. Arana, J.-M. Dona-Rodriguez, C. Garriga i Cabo, O. Gonzalez-Diaz, J.-A. Herrera-Melian, "FTIR study of gas-phase alcohols photocatalytic degradation with TiO<sub>2</sub> and AC-TiO<sub>2</sub>", *J. Perez-Pena, Appl. Catal. B: Env.*, vol. 53, pp. 221-232, 2004.